International Journal of Applied Mathematics
Volume 38 No. 10s, 2025
ISSN: 1311-1728 (printed version); ISSN: 1314-8060 (on-line version)

CRYSTALLIZATION AND MULTIFACETED CHARACTERIZATION OF L-ASPARAGINE MONOHYDRATE SINGLE CRYSTALS FOR STRUCTURAL, SPECTROSCOPIC, OPTICAL, THERMAL AND MORPHOLOGICAL ANALYSIS TOWARD FOR THIRD-ORDER NLO APPLICATIONS

N.Rajasekar[1], K. Balasubramanian[2*]

[1] Research scholar (Reg.No: 22211072131006), PG and Research department of physics, The M.D.T Hindu college, Pettai, Tirunelveli-627010, Tamil Nadu, India.

[2*]Associate professor, PG and Research department of physics, The M.D.T Hindu college, Pettai, Tirunelveli-627010, Tamil Nadu, India.

[1,2*]Affillated by Manonmaniam Sundarnar University, Abishekapatti-627012, Tirunelveli, Tamil Nadu, India.

Corresponding author*.

Correspondence: K. Balasubramanian

E-mail :*rs9012618@gmail.com

Abstract

L-Asparagine monohydrate (LAM) is grown by solution growth method is nucleation by the slow evapouration technique. Grown crystal has characterized by the various studies they are Powder XRD, FTIR, UV-vis, EDAX, CHN, Photoluminescence, 1H&13C FT-NMR, TG-DTA, SEM, LDT and Z scan. Powder XRD used to identify the Space group, Lattice parameters and crystal structure. X pert high score is the research tool which help to find the FWHM, Crystalline size and strain(η). FTIR is mainly identify the functional group of various assignments and Functional groups. DTA was used to study the thermal behaviour of the material, which provides insights into the stability and decomposition behaviour of the crystal under varying temperatures, including the determination of the glass transition temperature (TG). The thermal kinetic parameters such as Entropy(ΔS) j/mol.k, Enthalpy (ΔH) j/mol and Gibbs free energy (ΔG) j/mol is the technique which is used to find the Broidos method. In UV-Vis the optical property of the LAM compound which are find out the Transmittance (%), Linear Band gap (E_g) and Refractive index (n_o).The Z scan technique is generally helps for Third harmonic generation of Nonlinear absorption coefficient (β), Nonlinear refractive index (n2) and Third order susceptibility $X^{(3)}$.The LAM sample had the different elements of carbon, nitrogen, and oxygen, according to EDAX. Elemental analysis verifies the chemical makeup of growing samples. A Prominent peak in the Fluorescence spectrum, recorded from 200-800 nm, was seen at 467 nm. The LDT was experimentally determined as 24.8 GW/cm^2 . The FT-NMR method verified the molecular structure. The SEM image was captured the particle and minutes crack. SEM Reveals the information about growth quality and defect level.

Received: August 02 2025

International Journal of Applied Mathematics
Volume 38 No. 10s, 2025
ISSN: 1311-1728 (printed version); ISSN: 1314-8060 (on-line version)

Keywords: Powder XRD, FTIR, UV-vis, EDAX, TG-DTA, CHN, SEM, LDT, 1H & 13C FT-NMR, Photoluminescence and Z scan.

Introduction

L-Asparagine monohydrate (LAM) is an amino acid present in the human body and is considered one of the 20 amino acid. It also helps metabolize toxic ammonia in the body. LAM is the white crystalline powder which is soluable in deionized water as a solvent but not very soluable in methanol and ethanol. During literature survey, many research papers suggests that LAM crystals exhibits the Response to third harmonic generation (NLO), with the goal of aiding in the creation of effective materials for nonlinear optical technology**[1].** Additionally, the evaluation of third harmonic generation characteristics highlights the potential of LAM crystals in photonic, optical switching, and limiting applications. The primary component that promotes NLO appliances is a variety of amino acids **[2].** However, the LAM crystals feature a non-centrosymmetric space group and an asymmetric carbon atom. The chromophores are mostly found in the non-centrosymmetric space group. The term chromophores is present in the organic molecules which absorbs a light intensity and gives the different colors of wavelength**[3].**

Mostly the organic compound family group amino acid has excellent Nonlinear optical behaviour higher than the inorganic compound, Due to the reason of high polarizability. But in the LAM crystals examined low mechanical strength. The LAM crystal has good thermal and optical property. So that the LAM crystals was subjected into the different types of analysis which are Powder XRD, FTIR, UV-vis, SEM, EDAX, LDT, Photo-luminouscenes, CHN, TG-DTA, 1H & 13C FT-NMR and Z scan**[4].** Amino acids are most common examples of zwitterions they are made up of amino group which is made up of positive charge (+) as well as carboxyl group which consists of negative charge (-) which plays a important role in nonlinear optical property. Nonlinear optics effect responses that the frequency, polarization and path of intensity light. In third harmonic generation (THG), three incident photons interact to yield a single photon carrying triple the fundamental frequency, resulting in light with one-third of the wavelength **[5].** The title chemical was exposed to a powder XRD structure in the current investigation. The direct band gap energy was discovered in UV-vis. Z-scan has been used to calculate thermal parameters and third order nonlinearity.

Crystal Synthesis

To grow a LAM single crystals tends to polarization and nucleation at room temperature. To get beyond the LAM Sample, deionized water was added as a solvent.As we taken the LAM powder selected as pure (Extra pure CHR, 99%).

The molecular formula of the LAM single crystals is,

$C_4H_8N_2O_3. H_2O$

First step the LAM white crystalline powder was taken (5g) in our own beaker. In our sample synthesis we prepared the deionized water taken as a solvent. The (5g) of LAM powder was mixed with deionized water which makes until gets dissolved as the saturated solution. During 6 hours the solution gets continuously stirred into the magnetic stirrer. A solution was collected and

Received: August 02 2025

International Journal of Applied Mathematics
Volume 38 No. 10s, 2025
ISSN: 1311-1728 (printed version); ISSN: 1314-8060 (on-line version)

filtered using whatmann paper. The well prepared sample has been retrieved and crystallized within 30 days. The nucleation take time place in several days. The whole crystal growth experimental process was carried out by the slow evapouration method. The good optically transparent well shaped structural crystal was formed with the dimensions of 9mm x 8mm x 5mm. The crystals are depicted in the photograph shown in fig. (1)

Analytical techniques

The powder X Ray diffraction analysed by Bruker D8 Advance diffractometer were carried. The FTIR studies were carried out on a Bruker alpha II spectrometer using the KBr pellet technique in the range of 500-4500 cm^{-1}.Liquid UV-vis measurements were carried out with a JASCO V-730 spectrophotometer in the 190-1100 nm wavelength range. The obtained SEM-EDAX particle size and elements percentage were examined through Jeol 6390LA/OXFORD XMXN. LDT measurements were carried out using a Q- switched High energy (Nd:YAG) neodymium yttrium aluminium garnet Model: LAB-170_10) laser beam at 1064 Nanometers. In FT-NMR (^{1}H &^{13}C) for molecular structural Examined by the Model: Brukeravance III spectrometer (400 MHz for ^{1}H NMR & 400 MHz). TG/DTA of the grown crystals was analysed by using the instrument (SIINT 6300, Japan) to find the thermal stability of the crystal. The elemental composition (CHN) of the sample was determined using an Elementar, vario ELIII CHN analyzer. The (JASCO FP-8300 SPECTROFLUOROMETER) was employed for detailed Photoluminescence characterization. Third harmonic generation (THG) analysis was performed via the z scan technique with a 632.8 nm He-Ne laser.

Results and discussion

Powder XRD

Powder X-Ray diffraction is widely used to study structural properties for compounds like Phase identification, Crystal structure determination, Lattice parameter, Crystalline size and strain analysis. XRD detecting the presence of Intensity in the material, which can helps to find the high or low crystalline, impurity property and the behaviour**[6].**In the powder XRD we prepared the sample of L-asparagine monohydrate, where the Lab grown crystal was processed and crushed into a powdered form. Powder XRD which is mainly used for Crystal diffraction, phase identifications and then lattice parameters with a good agreement**[7]**.The dataset was acquired using CuαK radiation λ = 1.5418 A^{o} as the X- ray source. The LAM samples was scanned for the angular range 5^{o} – 10^{o}of 2θ with the increment of 0.05° min. Due to powder XRD analysis we find the LAM crystal has 87 % of high crystalline. The above grown samples of L-asparagine monohydrate has orthorhombic in structure which has an$P2_12_12_1$ space group. The theortical unit cell parameters for L-Asparagine monohydrate are a = 5.5963, b = 9.8407, c = 11.8076, V = 650.26 A°and the number of atoms Z = 4 and the interfacial angles are α= 90°,β = 90°, γ = 90. The various intensity's of diffracted peaks are corresponds to crystal lattice by the miller indices (1 1 0), (0 1 1), (1 0 1), (1 1 1), (2 1 1), (2 2 1), (1 3 1), (1 1 2), (3 3 0), (0 3 2),(4 0 1), (3 5 0), (3 3 2), (1 2 3) (H K L) planes are presented. The maximum intensity of the peaks are found to be (2 2 1) plane and then highest peak is produced as the 100 %.The powder XRD pattern of grown L-Asparagine monohydrate (LAM) matches standard data (JCPDS card no. 30-1529) taken via ICCD source.

Received: August 02 2025

International Journal of Applied Mathematics
Volume 38 No. 10s, 2025
ISSN: 1311-1728 (printed version); ISSN: 1314-8060 (on-line version)

PXRD plot depicting the LAM and the different (HKL) diffraction Peaks are denoted in a graph Fig.2.

FTIR technique

FTIR to determine the various assignments which including the Functional groups of an molecules. The FTIR measurements were performed in the range of 400 – 4000 cm^{-1} **[8].** Figure (3) depicts the plotted FTIR spectrum. A First peak observed at 509.17 cm^{-1} and then peak around 550.76 cm^{-1} is attributed to (COO rocking).A group of vibrations can be assigned to (COO^- bending vibration) lying between the 665.13 cm^{-1}.(C-C Stretching) at 800.29cm^1. (C-N Stretching) group observed at 1073.2 cm^{-1}. The ($NH3^+$ Rocking) group occured at 1148.6 cm^{-1}. Thus, the (C-COO)vibrations observed at 1237 cm^{-1}. A peaks obtained around 1307.1 cm^1 may due to (CH2 Bending modes) group. The 1356.5 $cm^{-1}$and also it includes at 1426.7 cm^{-1}peaks corresponds at (Symmetric COO^- Stretching). The (Asymmetric COO- Stretching) peaks at 1522.9 cm^{-1}. The peak identified in 1634.7 cm^{-1} the group presented is (C-N Stretching). A peak appearing near 2923.9 cm^{-1} is associated with (C-H Stretching). A peaks observed around 3100.6 cm^{-1} and 3376.2 cm^{-1} with the presented group is (N-H stretching vibration).

Liquid UV- vis analysis

The characterization of UV-visible spectroscopy is to Find wavelength, absorbance, Transmittance (%) and the linear Bandgap of the optical property **[9].** In LAM crystals, had optical transparency material which is good for laser applications. The LAM crystal has absorbance lower cut-off frequency at 244 nm. The sample exhibits the Transmittance at lower cut off wavelength 230 nm within UV visible wavelength range at 200nm to 800nm and the LAM crystals is in liquid solution Dissolved in deionized water was analyzed using a UV-vis spectrophotometer**[10].** LAM crystals indicate the 89 %Transparency which is clearly seen as a optical property.

The absorbance electronic transitions occurs between the (n-$\pi*$) which confirm the presence of -C=O (carbonyl) group in -$CONH_2$ (amide) group. LAM crystals of Transmittance had some electron transitions (n-$\pi*$) corresponds to the Carboxylate (-COO^-) group. The above sample transmittance 89 % shows the crystal is potential canditate for NLO applications. Thus, the sample 90% of transmittance in the 300 – 900nm range is good for Third harmonic generations**[11].** A Tauc plot is a graphical representation used to determine the optical bandgap energy (E_g) of a material. The Direct Bandgap of LAM crystals Tauc plot is found to be 5.70eV. The purpose of the extinction coefficient is to determine which chromophores—groups of atoms that absorb light—are involved **[12].** The percentage of light lost per unit distance in a given material as a result of scattering and absorption is known as the extinction coefficient. The value of refractive index was calculated n_o is 0.03

Photoluminescence analysis

Photoluminescence (PL) analysis is a valuable tool in the crystal growth process, especially for opto-electronics and nonlinear optical materials. The uses are Band gap determination, Defect and impurity analysis**.** The photoluminescence spectrum of LAM crystals depicted in fig (8). A maximum peak intensity was observed around 467 nm. The presence of (n-$\pi*$) and the group of-C=O (carbonyl) group in amide group (-$CONH_2$).This functional group can induce blue-region

Received: August 02 2025

International Journal of Applied Mathematics
Volume 38 No. 10s, 2025
ISSN: 1311-1728 (printed version); ISSN: 1314-8060 (on-line version)

emission in LAM crystals. The second peak obtained at 540 nm which is due to the (n-$\pi*$). The PL spectrum confirms that the material has potential in optoelectronics, Photonics and Nonlinear optical applications **[13].**The PL Spectrum exhibited its maximum emission peak around 467 nm. Using the wavelength (λ) nm to energy conversion(E_g), the Energy gap was calculated as 2.66 eV.

$$\mathbf{E_g = \frac{h \times C}{\lambda \times e}} \quad \textbf{(1)}$$

Where 'h', 'c', 'e' are standard values and 'λ' is wavelength. The other peaks observed arise from the due to anionic and cationic characteristics of the sample. The LAM exhibits blue emission at this wavelength. Excitation of the LAM sample at 467 nm produces the highest emission in the range of (200 to 900 nm), exhibiting a peak near 823 nm**[14].**

TG – DTA analysis

The Thermogravimetric and differential (TG - DTA) analysis performed in specific region with the nitrogen atmosphere from raising temperature upto 800° C at a specific heating rate of 20 ℃ per minute/ 0 min / 0.5 sec by using alumina. The sample that has taken for Thermogravimetric (TG) and Differential (DTA) analysis weighed measured in 5.543 mg

There are different types of phase transitions in TG - DTA analysis they are Melting, Vapourization, solid – solid transitions, Polymorphic transitions and Desorption these are occurred in Endothermic peak of TG curves**[15].**

The presence of Water molecules there is a majour weight loss TG - DTA graphs. In, DTA graph the sharp shallow exothermic peak formed at 98℃. The Endothermic peak was identified at 144℃corresponds to melting point or decomposition point signifying the additional decomposition and voltalization of the substance in a Differential Thermal analysis spectrum. The exothermic peak was observed around 220℃. The dehydrated crystal is thermally stable upto 252℃ Majour endothermic peak this proves that dehydration process does not destabilize the crystal structure. The minor Exothermic peak formed at 316℃ and then endothermic peak occurs at 359℃. The term Exothermic releases heat (peaks goes upward) and then Endothermic absorbs heat (Peaks goes downward) in DTA uV curve.

In TG curves the first stage of decomposition occurs at around 100℃, where the sample loses of water molecules through evaporation. The second decomposition stage at 119℃ results in the liberation of one molecule of water (H_2O), indicating dehydration of the compound. The third - weight loss stage near around 232℃ arises from thermal decomposition of the organic moiety, accompanied by the release of ammonia (NH_3) and carbondioxide (CO_2) as a result of deamination and decarboxylation reactions. After elimination of the amine moiety, the compound destabilizes and libearates the C_2H_2 group at around 262℃. The temperature range of weight loss is 375℃ which is elimination of HCOH group**[16]**. The sharp peak indicates the purity and crystallinity nature of the material **[17]**.This TG graph shows the weight loss of wide range of temperature between 100 – 380℃."Due to Thermal analysis this compound is mainly suitable for Nonlinear optical applications.

Received: August 02 2025

International Journal of Applied Mathematics
Volume 38 No. 10s, 2025
ISSN: 1311-1728 (printed version); ISSN: 1314-8060 (on-line version)

The Broido method was employed to evaluate the kinetic parameters-namely, activation energy, enthalpy of activation (ΔS) j/mol/k, entropy of activation (ΔH) j/mol, and gibbs free energy (ΔG) j/mol, corresponding to the second stage of thermal decomposition**[18].**

Z Scan liquid analysis

The Z Scan method is implemented to analyze the third harmonic generation characteristics of materials, including their nonlinear refractive index (n2) and adsorption coefficient (β). It involves scanning a focused beam through a sample liquid while measuring the transmitted light. The Third order is typically detected using a Photomultiplier tube. Z scan is highly sensitive to nonlinear optical effects, making it deal for detecting THG signals. Z scan setup is regarded as basic and accessible for implement.

The sweeping distance, measured perpendicular to the laser beam, is the total distance the sample moves along the z axis. The sweeping distance typically ranges from 1-20 mm. The sweeping for LAM sample is 10mm. The step distance to the z scan analysis is 0.25mm. The step distance is refers to the incremental distance by which the liquid specimen is displaced along the z-axis. In (THG) the bandwidth refers to the range of frequencies over which the applied laser source irradiates the speciemen. The observed bandwidth is high. “The laser beam interacts with the sample, inducing NLO effects, the beam of laser light interact with sample and then produce the different wavelength. The wavelength of laser beam is usually measured in nanometers (nm). The wavelength (λ) of LAM sample is 632.8 nm. The power of the laser can vary from milliwatts (mW) to watts (W). The Power of the laser (Ep) is 0.012 Mw. The diameter of the laser beam refers to the width of the laser beam at the point where it interacts with the liquid sample. The Diameter of the laser beam (d) is 5 mm. The focal length of the convex lens is distance between the lens and the point where the laser beam focused to the smallest diameter. The Focal length of the lens (f) is 200mm and the radius of the aperture 2mm and the radius of the beam at aperture (Wa) is 4.5 mm. In Z scan the LAM sample thickness (L) was measured in 1mm, with a observed value of Rayleigh length (ZR) of 1.288 mm. The condition was satisfied when (L<ZR) **[19].**

In closed aperture configuration the nonlinear third order refractive index (n2) value was found to be 1.91 x 10^{-11} m^2/W. Under the open aperture the configuration, the absorption coefficient (β) that I found to be 5.45 x 10^{-2} m/W for LAM single crystals. The real part of susceptibility noted as 4.34 x 10^{-11} esu, thus the imaginary part of susceptibility is 8.74 x 10^{-4}esu. The magnitude of the third order susceptibility $X^{(3)}$ notified as 8.74 x 10^{-4}esu for LAM**[20].** The open aperture for the Z scan technique graph was plotted in Fig.12(a). The closed aperture for the Z scan analysis datas plotted in Fig.12(b).

The value of β is for saturable absorption and for two photon absorption. The Third order non linear refractive index and the nonlinear absorption coefficient were evaluated from the Z scan measurements.

The calculated value of nonlinear refractive index n_2 is 4.57 x 10^{-3} m^2/W. In the closed aperture Z-scan, if the normalized transmittance shows a valley followed by a peak, it indicates self-focusing behaviour with a positive nonlinear refractive index ($n_2 > 0$). From the open curve z scan nonlinear absorption coefficient (β) is found to be 1.01 x 10^{-1} m/W. The open aperture Z-scan

Received: August 02 2025

International Journal of Applied Mathematics
Volume 38 No. 10s, 2025
ISSN: 1311-1728 (printed version); ISSN: 1314-8060 (on-line version)

curve shows a symmetric peak around the focal point (z=0), indicating saturable absorption (RSA) behavior and a negative nonlinear absorption coefficient ($\beta < 0$)."

The real part has been determined to be 7.51 x 10^{-6}esu. The Imaginary part is calculated as 8.27 x 10^{-2}esu. The magnitude of third order susceptibility determined to be 8.27 x 10^{-2}esu**[21].**

CHN Analysis

The CHN analysis is a commonly used technique in materials chemical composition to determine the percentage of the following elements in a compound. For analysis purpose 4.54 mg sample was taken for each C, H and N to find the weight (%).The experimentally determined percentage of C, H and N were compared with theoretical values computed on the basis of the chemical formula of the synthesized compound. The elemental percentage are Carbon (30.90 %), Hydrogen (17.76 %) and Nitrogen (3.79 %) are measured. The Theortical (%) and experimental (%) results are displayed within Table (2). The molecular formula of L-Asparagine monohydrate is $C_4H_{10}N_2O_4$. The chemical structure of L-Asparagine monohydrate is illustrated in Figure (13). The theoretical (%) using the molecular formula and compare it with the experimental (%) that we obtain from elemental analysis**[22]**.

EDAX characterization

EDX in SEM determined the elemental composition of NLO crystals. SEM - EDS detects impurities and their distribution within the crystal. The LAM samples shows the presence of carbon, Nitrogen and oxygen are shown Table (3). EDS is widely used technique for phase identification in SEM. It involves analyzing the X-Ray emitted by the sample when excited by the electron beam. In EDX analysis, the K shell, which is the innermost electron shell closest to the nucleus, contributes significantly to the generation of characteristic X-rays, which are used to determine the chemical composition of a compound. When accelerated electrons strike a sample, they can eject inner-shell electrons from target atoms, creating vacancies in the K-shell. The energy and intensity of the X-rays are employed to examine the elements present in the crystal **[23].** There are some various elements present in the LAM sample are carbon, Nitrogen and oxygen. In EDAX (Energy dispersive X-ray analysis) carbon, Nitrogen and oxygen are considered light elements. They are classified as light elements due to their low atomic numbers (Carbon : 6, Nitrogen : 7, Oxygen : 8). Thus, the Carbon Nitrogen and Oxygen are essential components in NLO materials such as organic crystals. The applications which are used for photonic devices such as optical switches, modulators and wavelength converters. Fig (14) diagram shows analyses the positions and intensities of these peaks, researchers can determine the atoms contained within the LAM material **[24].**

^{1}H and ^{13}C FT-NMR analysis.

Among, the LAM ^{1}H signals at 3.867, 3.856, 3.848, 3.837 ppm are due to the (methyl group) α-CH (Asparagine) amino group present in the compound which split into quartet. The signals at δ = 2.825, 2.814, 2.783, 2.772, 2.730, 2.711, 2.688 and 2.669 ppm which corresponds to the presence of (Methylene) group of β-CH_2 (Asparagine) group (Doublet). The ^{1}H FT-NMR spectrum is presented in fig.15 (a), Fig.15 (b) and fig.15 (c) and Deuterium (D2O) as a solvent.

Received: August 02 2025

International Journal of Applied Mathematics
Volume 38 No. 10s, 2025
ISSN: 1311-1728 (printed version); ISSN: 1314-8060 (on-line version)

The LAM FT-NMR ^{13}C signals at 34.39 ppm attributed to the presence of β- (CH_2) (Asparagine). The Signals was observed at 51.8 ppm associated to the existence of α- CH (Asparagine). A signal at 173.23 ppm are due to (COOH (Carboxyl carbon) and then 174.34 ppm which corresponds to the $CONH_2$ (Amide Carbonyl). The ^{13}C FT-NMR spectra are plotted in Fig. 15 (d). The LAM FT-NMR ^{13}C of (D2O) Deuterium is used as the solvent **[25].**

Laser damage threshold (LDT) analysis

The laser-induced damage threshold was evaluated using a Q-switched Nd:YAG laser source operating at a wavelength (λ) of 1064 nm with a pulse width (τ) duration of 10 ns. The laser operated at a repetition rate of 10 Hz. A laser beam of 1 mm diameter was focused onto the crystal surface using a convex lens with a focal length (f) of 10 cm. The input pulse energy was precisely monitored with a QUANTA-Ray power meter (Model No. 170-10). The output energy of the laser was measured E_p as 21.5 mJ.

The equation for Power density

$$\mathbf{(P_d) = E_P/ \tau\pi(\omega_0)^2\ (GW/cm^2)} \qquad \mathbf{(2)}$$

The L-Asparagine monohydrate material produce the Calculated LDT value observed at 24.8 GW/cm^2 respectively these values are significantly higher than KDP reference material." The L-Asparagine monohydrate (LDT) calculated and observed values are mentioned in the table: (5).

I literature reviewed in L-Asparagine Tartarate research papers taken as reference material of standard (KDP) value in Laser damage threshold is 0.2 GW/cm^2 **[26].**

Optimized crystal LDT analysis informs crystal growth parameters, leading to improved crystal quality and performance. LDT testing helps identity crystal damage mechanics, enabling the development of more resistant crystals. The damaged crystal by a induced laser beam is really a suitable for LDT. LDT analysis helps to prevent crystal damage, ensuring reliable operation in various NLO applications. By understanding the damage threshold, researchers can optimize material processing. The laser parameters helps to find the pulse duration and wavelength. A High power laser pulse is passed through the crystal. Thus the crystal absorbs the laser beam and the localized temperature increase when the temperature increase leads to heat expansion that cause the crystal lattice. Due to heat expansion the stress exceeds the material damage threshold. LDT is measured by incrementing the laser fluence until damage is detected **[27].**

In, LDT there are several ranges of power density (P_d) the factors influencing widely used for variety of Advanced NLO applications such as THG, Optical parametric oscillators and All optical switching.

Scanning electron microscopy.

SEM employs a finely focused electron beam to examine the surface morphology of crystal, creating high resolution images in fig 16 (a) and fig 16 (b). SEM is primarily used for surface analysis, allowing researchers to observe the texture and structure in organic samples on a microscopic scale. Scanning electron microscopy is the characterization for studying surface morphology, Roughness, Fractal dimension structure, size and shape of crystals. SEM can be used to analyze the particle size distribution of powder grains. SEM analyses the grain size and

Received: August 02 2025

ISSN: 1311-1728 (printed version); ISSN: 1314-8060 (on-line version)

orientation in polycrystalline NLO materials, affecting the optical properties. Secondary electron (SE) imaging is commonly used for organic materials, as it yields high- resolution imaging of the sample's surface morphology. Backscattered electron (BSE) imaging can provide information on the sample's composition and structure. Low voltage SEM operating the SEM at lower voltages (e.g 1-5 kV) can help reduce radiation damage and charging effects. There are several applications in powder form crystals SEM analysis is morphology analysis, particle size distribution and surface feature analysis. Scanning electron microscopy (SEM) is used in the study of Nonlinear optical (NLO) crystals to analyze their surface morphology, identify defects and assess the quality of grow crystal. SEM provides High-resolution image of the crystal surface, that used to observe features like grain boundaries. SEM is used in the study of surface morphology, identify defects and analyze elemental composition and potential for NLO applications **[28].** SEM Image explore the irregular shape of grown LAM crystals **[29]**. The LAM layer exhibits a fine multilayered, plate like morphology along with minor cracks and a few microcrystals visible on the crystal surface **[30].**

Conclusion

The LAM crystals were fabricated using the solution growth method gradual evaporation technique. In PXRD analysis shows the space group of $P2_12_12_1$ with orthorhombic structure. The various functional group and Assignments are characterized by the FTIR studies. In, UV-visible studies the Transmittance (77%), are denoted in the plotted graph. The Crystal indicates the Transmittance at lower cut off frequency 230 nm within the UV visible wavelength range at 200nm to 800nm. The Linear bandgap energy is determined as 5.70 eV. The refractive index of the UV-vis is calculated by the no =0.03. The EDAX recorded was find out the different types of elements such as Carbon, Nitrogen and Oxygen. In CHN analysis carbon 30.90 %, Hydrogen 3.79 % and Nitrogen 17.76 % is a type of elemental analysis used in crystal growth studies to confirm the elemental composition and purity of an organic material. The thermal parameters of different phases. TG-DTA shows the material thermally stable upto 98℃ and also the kinetic parameters also calculated. Furthermore the Real $X^{(3)}$ (esu) value is 7.51 x 10^{-6}esu and imaginary part $X^{(3)}$ (esu) value is 8.27 x 10^{-2}esu. The calculated third order susceptibility $X^{(3)}$ (esu) is 8.27 x 10^{-2}esu, Nonlinear refractive index of (n2) is 4.57 x 10^{-3} m^2/W and also the Nonlinear Absorption coefficient (β) is 1.01 x 10^{-1} m/W. The observed emission maximum peak 467nm correspond to confirmed the blue light emission. These PL results demonstrate the potential of the synthesized crystal for applications in opto electronic devices and Nonlinear optical technologies. SEM image of LAM sample crystals reveal surface morphology and particle size. An obtained 1H FT-NMR profile of the synthesized L-Asparagine monohydrate shows characteristic chemical shifts at 3.8 ppm (α- CH), 2.6-2.8 ppm (β-CH_2). The 13C FT-NMR spectrum displays signals at 51.0 – 53.0 ppm (α- CH), 35.0 -37.0 ppm (β– CH_2), 175.0 -177.0 ppm ($CONH_2$), 173.0-175.0 ppm (COOH) corresponding to the Asparagine groups. The laser damage threshold (LDT) calculated L-Asparagine monohydrate sample is 24.8 GW/cm^2.

ACKNOWLEDGEMENT

"I sincerely thank my guide, Dr. K. Balasubramanian of The M.D.T Hindu college, Tirunelveli, for his constant support and guidance throughout my research work".

ISSN: 1311-1728 (printed version); ISSN: 1314-8060 (on-line version)

References

[1] R.C. Santana, H.O. Gontijo, A.F. Menezes, J.A. Martins, J.F. Carvalho, The effect of CuII ions in L-asparagine single crystals, Phys. B Condens. Matter. 501 (2016) 84–89. https://doi.org/10.1016/j.physb.2016.08.007.

[2] S. Sylvestre, S. Sebastian, S. Edwin, M. Amalanathan, S. Ayyapan, T. Jayavarthanan, K. Oudayakumar, S. Solomon, Vibrational spectra (FT-IR and FT-Raman), molecular structure, natural bond orbital, and TD-DFT analysis of l-Asparagine Monohydrate by Density Functional Theory approach, Spectrochim. Acta - Part A Mol. Biomol. Spectrosc. 133 (2014) 190–200. https://doi.org/10.1016/j.saa.2014.05.040.

[3] K. Thukral, N. Vijayan, D. Haranath, V. Jayaramakrishnan, J. Philip, P. Sreekanth, G. Bhagavannaryana, Assessment on third order non linearity and other optical analyses of l-Asparagine Monohydrate single crystal: An efficient candidate for harmonic conversions, Spectrochim. Acta - Part A Mol. Biomol. Spectrosc. 151 (2015) 419–425. https://doi.org/10.1016/j.saa.2015.05.051.

[4] A.S. De Menezes, F.M. Ardito, A.O. Dos Santos, A.J.D. Moreno, R.J.C. Lima, M.A. Hayashi, L.P. Cardoso, Characterization of the time-dependent l-asparagine monohydrate crystal phase transition, J. Appl. Crystallogr. 44 (2011) 954–957. https://doi.org/10.1107/S002188981103322X.

[5] M. Shakir, S.K. Kushawaha, K.K. Maurya, S. Kumar, M.A. Wahab, G. Bhagavannarayana, Enhancement of second harmonic generation, optical and dielectric properties in l-asparagine monohydrate single crystals due to an improvement in crystalline perfection by annealing, J. Appl. Crystallogr. 43 (2010) 491–497. https://doi.org/10.1107/S0021889810008745.

[6] M.A. Rahman, J. Podder, Growth of L-asparagine monohydrate organic single crystals: An experimental and DFT computational approach for nonlinear optical applications, Heliyon. 10 (2024) e39842. https://doi.org/10.1016/j.heliyon.2024.e39842.

[7] A. Gupta, M.K. Raseel Rahman, R.O.M.U. Jauhar, V. Sivasubramani, N. Vijayan, G. Vinitha, L. Nair, Growth of L-asparagine monohydrate and its structural, optical, mechanical, thermal and electrical studies for nonlinear optical applications, Mater. Res. Express. 6 (2019). https://doi.org/10.1088/2053-1591/ab7a5d.

[8] R. Subaranjani, J. Madhavan, M. Victor Antony Raj, Density functional theoretical and experimental investigation on l-asparaginium picrate-A nonlinear optical material, Mater. Today Proc. 8 (2019) 108–116. https://doi.org/10.1016/j.matpr.2019.02.087.

[9] S. Tamilselvan, M. Vimalan, I. Vetha Potheher, R. Jeyasekaran, F. Yogam, J. Madhavan, Generation of 532 nm laser radiation and phase matching properties of organic nonlinear optical material, Optik (Stuttg). 125 (2014) 164–169. https://doi.org/10.1016/j.ijleo.2013.06.024.

Received: August 02 2025

ISSN: 1311-1728 (printed version); ISSN: 1314-8060 (on-line version)

[10] N. Suresh, J. Arumugam, R. Ragavendiran, S. Karthikeyan, M. Selvapandiyan. Growth and characterizations of L-Asparagine single crystals. JETIR, December 2018, Volume 5, Issue 12 .www.jetir.org (ISSN-2349-5162). DOI: 10.1729/Journal.19228

[11] M. Shkir, S. Muhammad, S. Alfaify, A. Irfan, I.S. Yahia, A dual approach to study the electro-optical properties of a noncentrosymmetric l-asparagine monohydrate, Spectrochim. Acta - Part A Mol. Biomol. Spectrosc. 137 (2015) 432–441. https://doi.org/10.1016/j.saa.2014.08.033.

[12] M. Shakir, B. Riscob, K.K. Maurya, V. Ganesh, M.A. Wahab, G. Bhagavannarayana, Unidirectional growth of l-asparagine monohydrate single crystal: First time observation of NLO nature and other studies of crystalline perfection, optical, mechanical and dielectric properties, J. Cryst. Growth. 312 (2010) 3171–3177. https://doi.org/10.1016/j.jcrysgro.2010.07.061.

[13] M. Saravanan, A. Senthil, S.A. Rajasekar, Growth and characterization of proficient second order nonlinear optical material: L-asparaginium picrate (LASP), Opt. Laser Technol. 83 (2016) 67–75. https://doi.org/10.1016/j.optlastec.2016.03.026.

[14] R.H. Rao, S. Kalainathan, Spectroscopic investigation, nucleation, growth, optical, thermal and second harmonic studies of novel semi-organic nonlinear optical crystal-Thiourea urea zinc sulfate, Spectrochim. Acta - Part A Mol. Biomol. Spectrosc. 97 (2012) 456–463. https://doi.org/10.1016/j.saa.2012.06.033.

[15] K.R. Raj, P. Murugakoothan, Effect of Co2+ on the growth and physical properties of potential nonlinear optical l-Asparaginium picrate crystal, Optik (Stuttg). 124 (2013) 2696–2700. https://doi.org/10.1016/j.ijleo.2012.08.032.

[16] F. Yogam, I. Vetha Potheher, R. Jeyasekaran, M. Vimalan, M.A. Arockiaraj, P. Sagayaraj, Growth, thermal, and optical properties of l-asparagine monohydrate NLO single crystal, J. Therm. Anal. Calorim. 114 (2013) 1153–1159. https://doi.org/10.1007/s10973-013-3138-8.

[17] K. Naseema, S. Ravi, R. Sreedharan, Studies on a novel organic NLO single crystal: L-asparaginium oxalate, Chinese J. Phys. 60 (2019) 612–622. https://doi.org/10.1016/j.cjph.2019.05.037.

[18] S. Manikandan, R. Mahalakshmi, P. Krishnan, F. Yogam, P. Rajesh, Growth, structural, optical, thermal and dielectric properties of l-asparagine monohydrate admixtured l-thiomalic acid single crystal, Optik (Stuttg). 127 (2016) 5316–5321. https://doi.org/10.1016/j.ijleo.2016.03.036.

[19] T.C. Sabari Girisun, S. Dhanuskodi, Linear and nonlinear optical properties of tris thiourea zinc sulphate single crystals, Cryst. Res. Technol. 44 (2009) 1297–1302. https://doi.org/10.1002/crat.200900351.

[20] S. Vediyappan, A. Raja, R.M. Jauhar, R. Kasthuri, V. Vijayan, M.S. Pandian, R. Perumalsamy, V. Gandhiraj, Synthesis, crystal growth, structure, crystalline perfection, thermal, linear, and nonlinear optical investigations on 2-amino-5-nitropyridine 4-chlorobenzoic acid (1:1): a novel organic single crystal for NLO and optical limiting

Received: August 02 2025

ISSN: 1311-1728 (printed version); ISSN: 1314-8060 (on-line version)

applications, J. Mater. Sci. Mater. Electron. 32 (2021) 15026–15045. https://doi.org/10.1007/s10854-021-06056-5.

[21] S.A. Avila, A.L. Rajesh, Linear and Nonlinear Optical Properties of L-Alanine Oxalate Single Crystals, 16 (2016) 125–134.

[22] K.J. Arun, S. Jayalekshmi, Growth and Characterisation of Nonlinear Optical Single Crystals of L-Alaninium Oxalate, J. Miner. Mater. Charact. Eng. 08 (2009) 635–646. https://doi.org/10.4236/jmmce.2009.88055.

[23] P. Kathiravan, T. Balakrishnan, Growth and Characterization of Pure and Cesium - Doped L - Asparagine Monohydrate Single Crystals, Struct. Chem. Crystallogr. Commun. 1 (2015) 1–9. https://doi.org/10.21767/2470-9905.100009.

[24]. M. K. Sangeetha, M. Mariappan, G. Madhurambal, S. C. Mojumdar, TG–DTA, XRD, SEM, EDX, UV, and FT-IR spectroscopic studies of L-valine thiourea mixed crystal, J Therm Anal Calorim, 4th September 2014DOI : 10.1007/s10973-014-4123-

[25]. S. Dhanushkodi and K. Vasantha. Structural, Thermal and optical characterizations of a NLO material: L-Alanium oxalate. Crystal Research technology, 39, NO 3, 259-265 (2004), DOI : 10.1002/crat.200310180

[26]. P. Vivek et al. Linear and Nonlinear optical property of a new organic NLO L-Asparaginum tartarate (AST) single crystal Optik (2013). DOI :http://dx.doi.org/10.1016/j.ijleo.2012.12.004

[27]. P. Jeyaprakash, P. Sangeetha, C. RathikaThayakumari, I. Baskaran, M. Lydlacaroline. Growth and characterization of L-Asparagine monohydrate admixture DL- Mandelic acid nonlinear optical single crystal.J Mater Sci: Mater Electron (2017).DOI : 10.1007/s10854-017-7828-z

[28]. B. Deepa, P. Philominathan, Investigation on the optical, mechanical and magnetic properties of organic NLO single crystal : Pyridine 3- carboxylic acid, Optik – International journal of light and electron optics, (2016), DOI :http://dx.doi.org/doi:10.1016/j.ijleo.2016.06.073

[29]. D. Jini et al. Structural, Optical, and Biological Properties of L-Alanine single crystal by slow evapouration method. Materials today : proceedings, 43 (2021) 2032-2035 DOI :https://doi.org/10.1016/j.matpr.2020.11.736

[30]. N. Rajasekar, K. Balasubaramanian, Exploring structural, spectroscopic, Optical, Morphological, Mechanical, Antibacterial and Thermal parameters of Glycine A.R single crystals for advanced opto electronics, Photonics, Laser components and Nonlinear optical applications. Journal of nanotechnology perceptions (www.nano-ntp.com). 20 No. S 14 (2024), 4857-4893. ISSN 1660-6795. DOI : https://doi.org/10.62441/nano-ntp.vi.5784

Received: August 02 2025

International Journal of Applied Mathematics
Volume 38 No. 10s, 2025
ISSN: 1311-1728 (printed version); ISSN: 1314-8060 (on-line version)

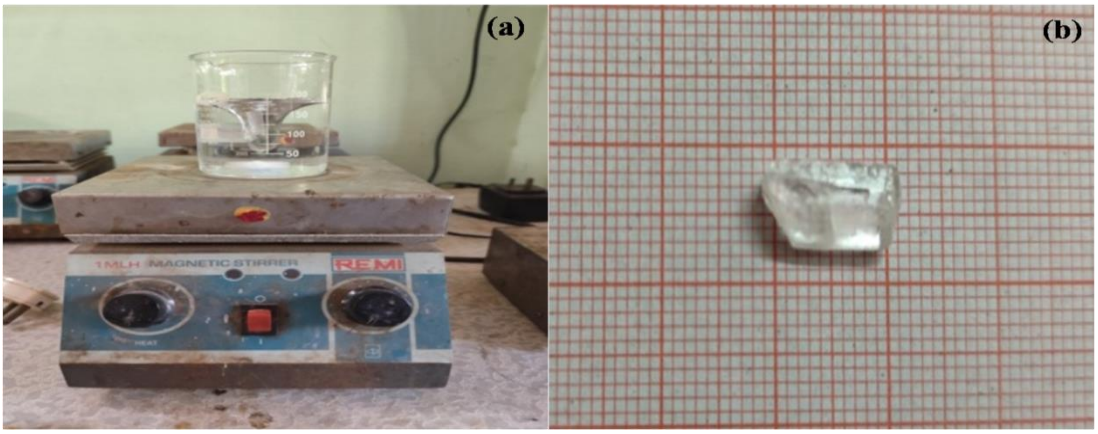

Fig. 1 Photographic image of (a) preparation setup of LAM crystal and (b) LAM crystal

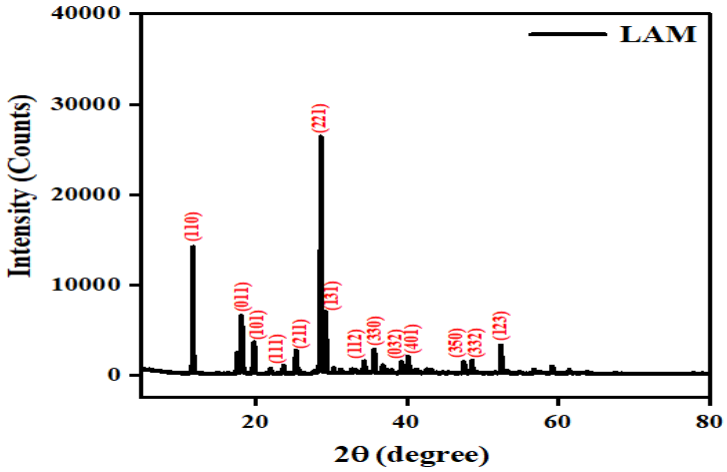

Fig. 2 Powder X-ray diffraction pattern of LAM crystal

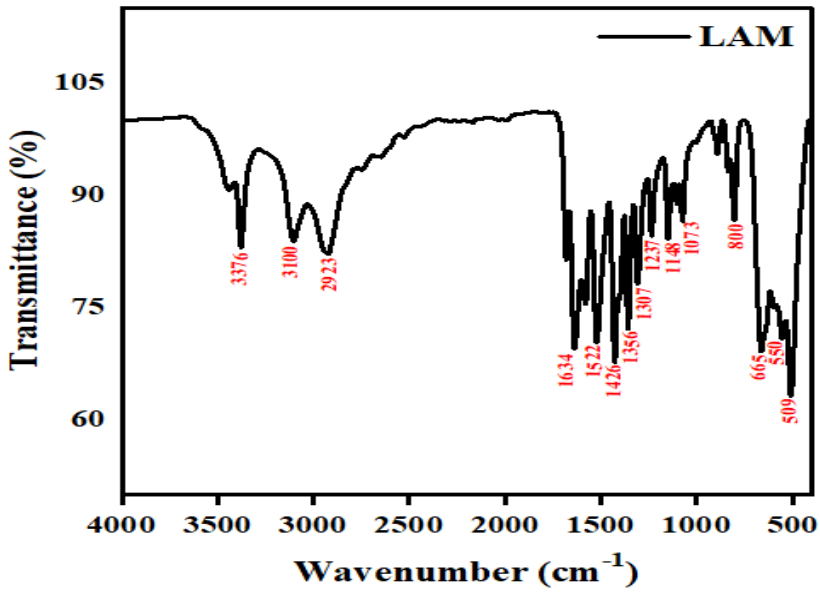

Fig.3 Fourier Transform infrared Spectroscopy plot of LAM crystal

Received: August 02 2025

International Journal of Applied Mathematics
Volume 38 No. 10s, 2025
ISSN: 1311-1728 (printed version); ISSN: 1314-8060 (on-line version)

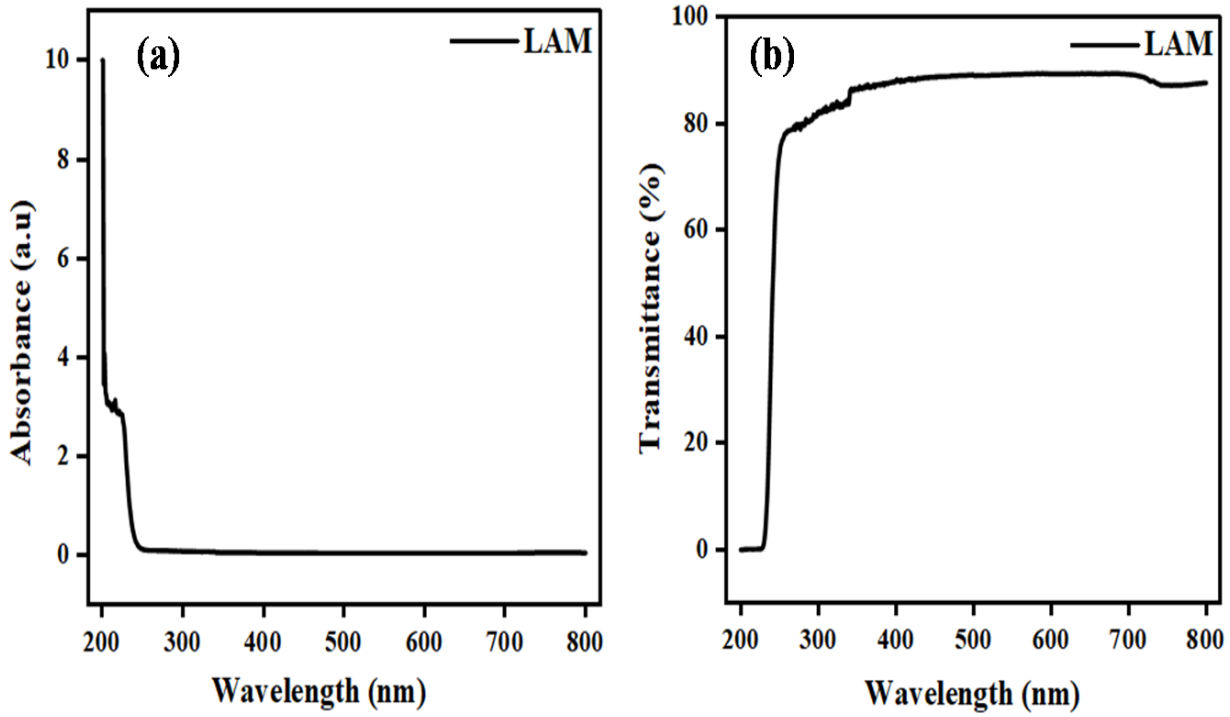

Fig. 4 Optical behaviour of LAM crystal (a) absorbance (b) Transmittance

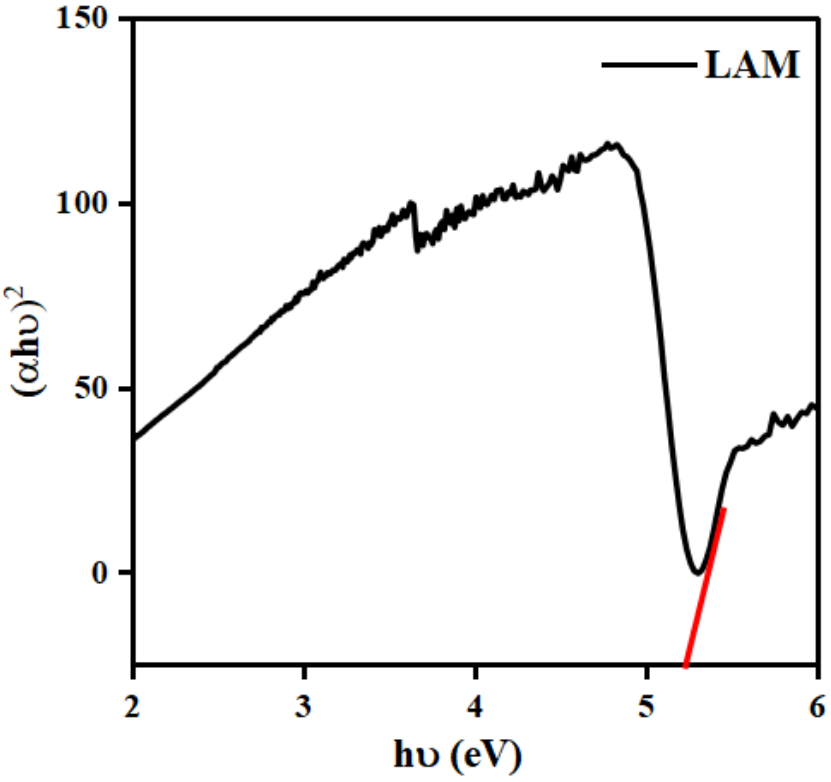

Fig. 5 Taue plot of LAM crystal

Received: August 02 2025

International Journal of Applied Mathematics
Volume 38 No. 10s, 2025
ISSN: 1311-1728 (printed version); ISSN: 1314-8060 (on-line version)

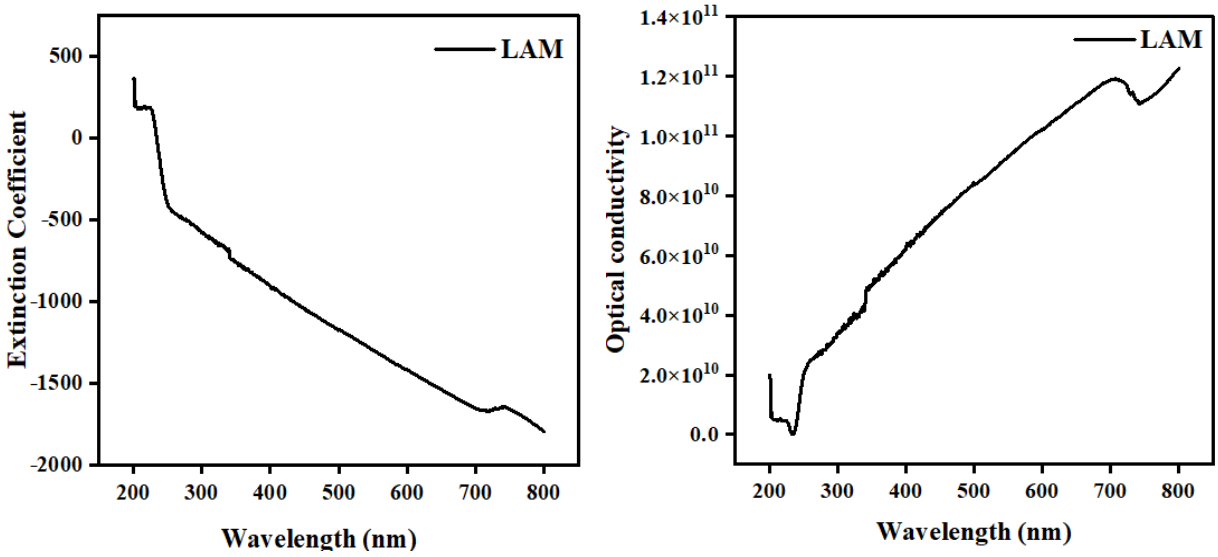

Fig. 6 Optical behaviour of LAM crystal **(a)** Extinction coefficient and **(b)** Optical conductivity

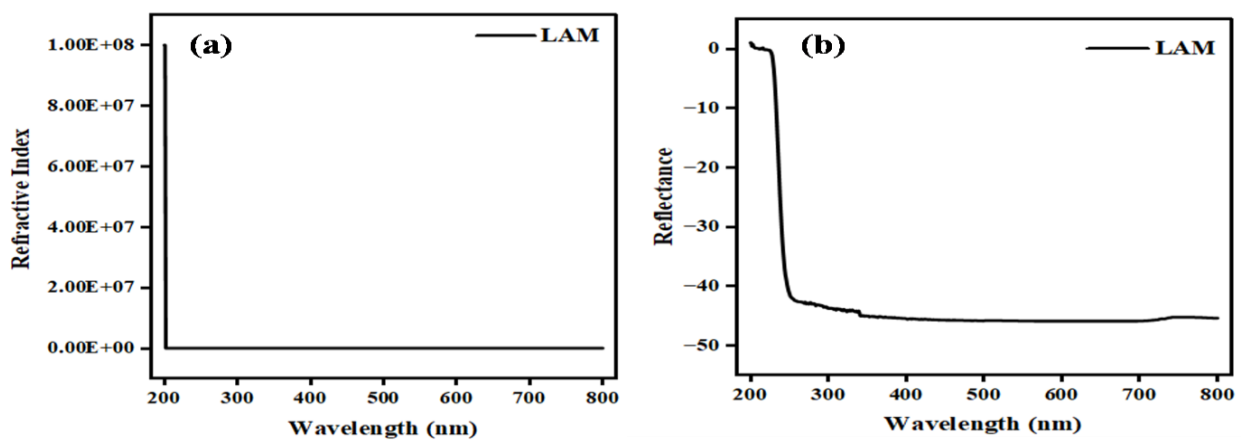

Fig. 7 Optical behaviour of LAM crystal **(a)** refractive index and **(b)** Reflectance

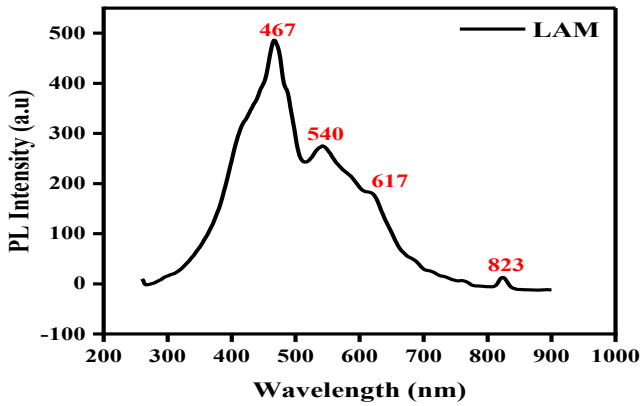

Fig. 8 Photo-luminance Spectra of LAM crystal

Received: August 02 2025

International Journal of Applied Mathematics
Volume 38 No. 10s, 2025
ISSN: 1311-1728 (printed version); ISSN: 1314-8060 (on-line version)

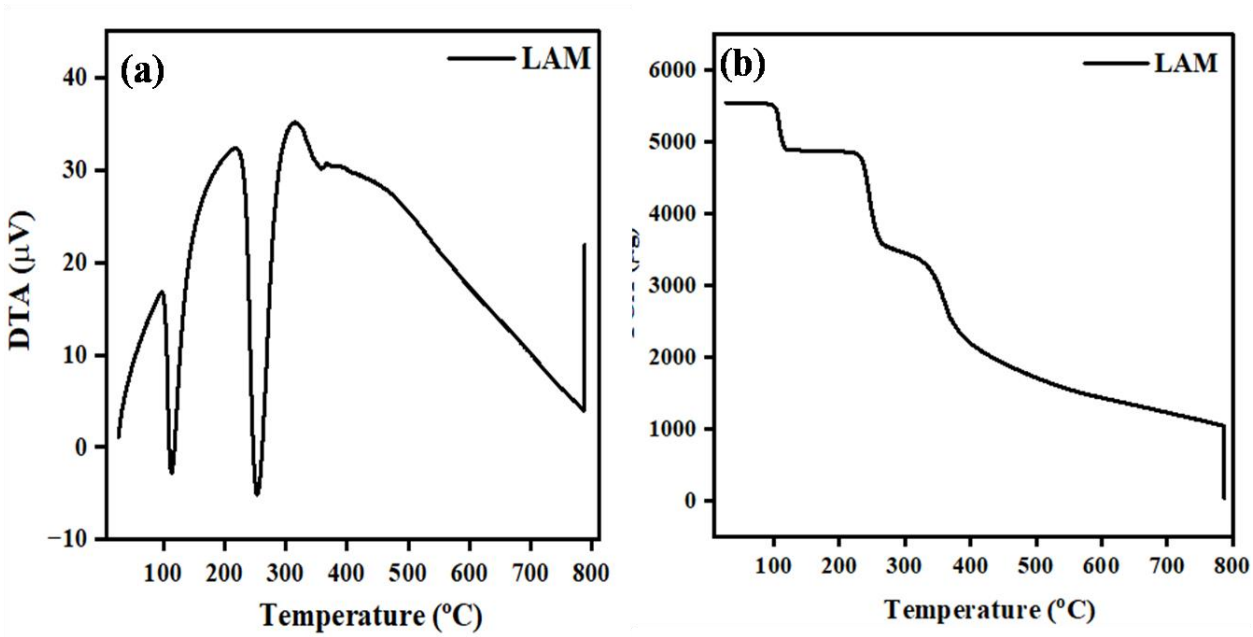

Fig. 9 Thermal behaviour of LAM crystal (a) plot of DTA and (b) plot of TGA

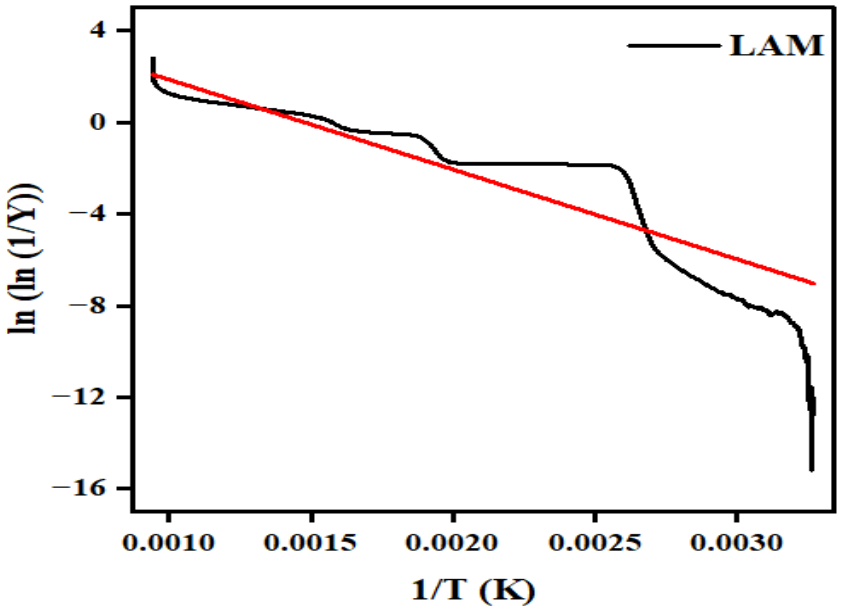

Fig. 10 Thermal behaviour of LAM crystal the Broidos method plot

Received: August 02 2025

International Journal of Applied Mathematics
Volume 38 No. 10s, 2025
ISSN: 1311-1728 (printed version); ISSN: 1314-8060 (on-line version)

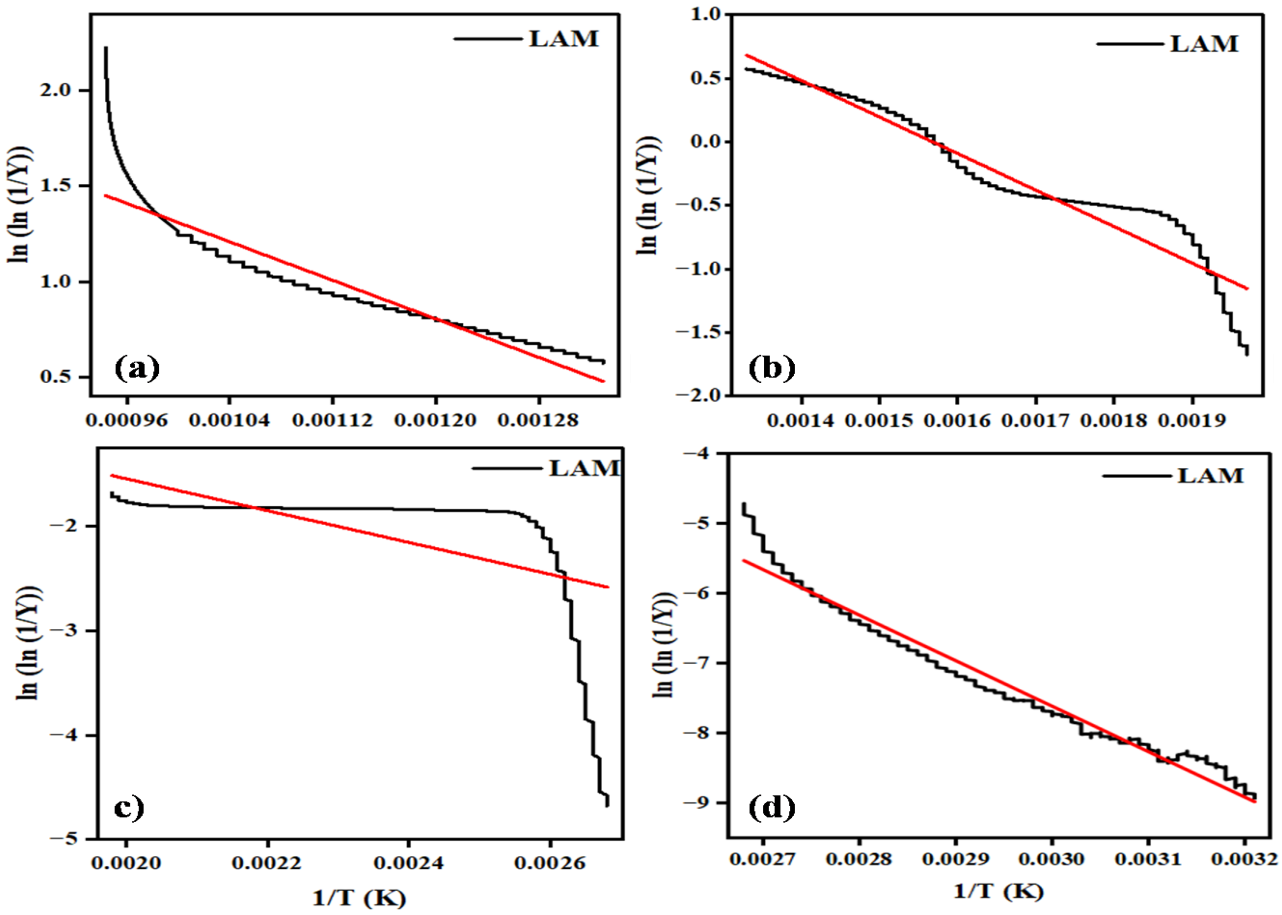

Fig. 11 The Broidos method plot of LAM crystal with various temperatures **(a)** Temp_1, **(b)** Temp_2, **(c)** Temp_3 and **(d)** Temp_4

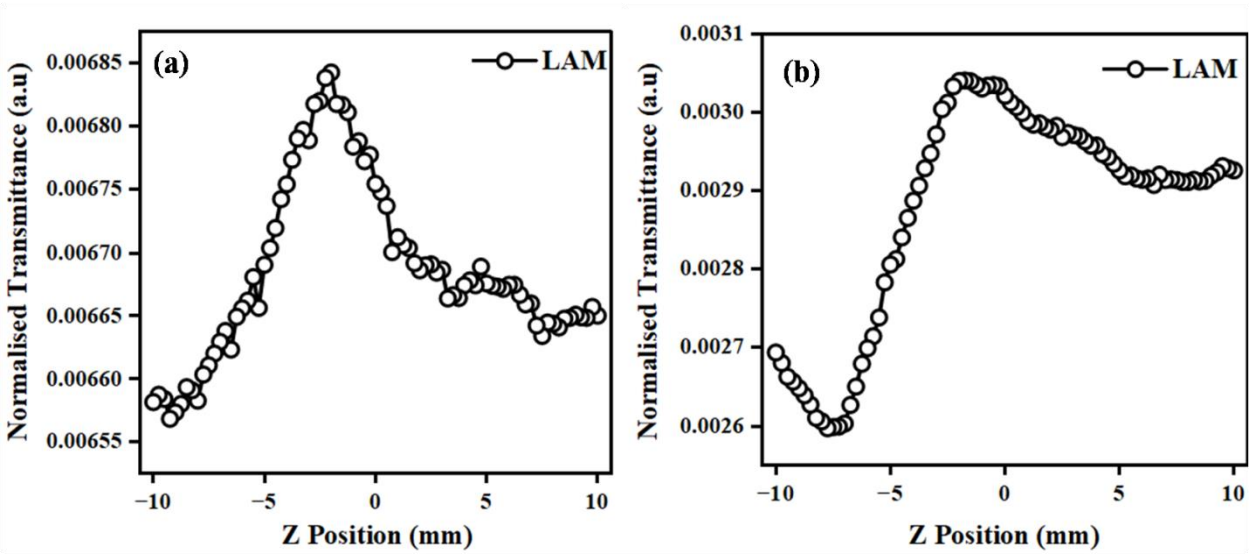

Fig. 12 Z position plot of LAM crystal **(a)** Open aperture and **(b)** Closed aperture

Received: August 02 2025

International Journal of Applied Mathematics
Volume 38 No. 10s, 2025
ISSN: 1311-1728 (printed version); ISSN: 1314-8060 (on-line version)

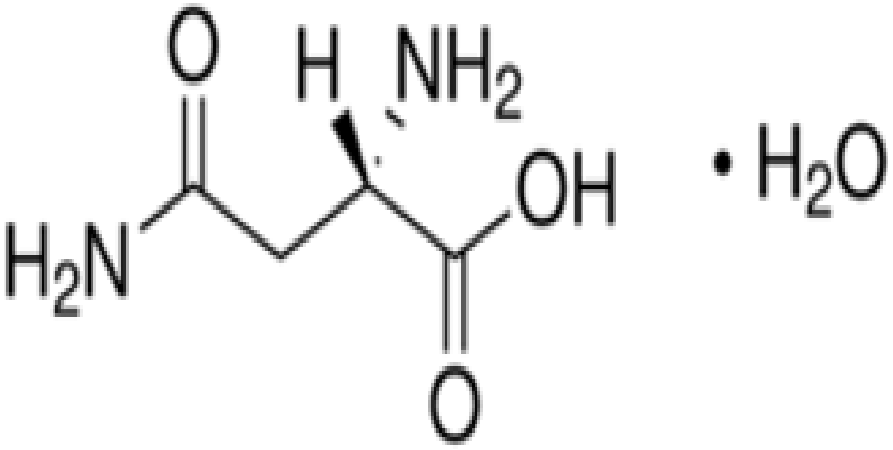

Fig.13. Moleculare structure of LAM crystal

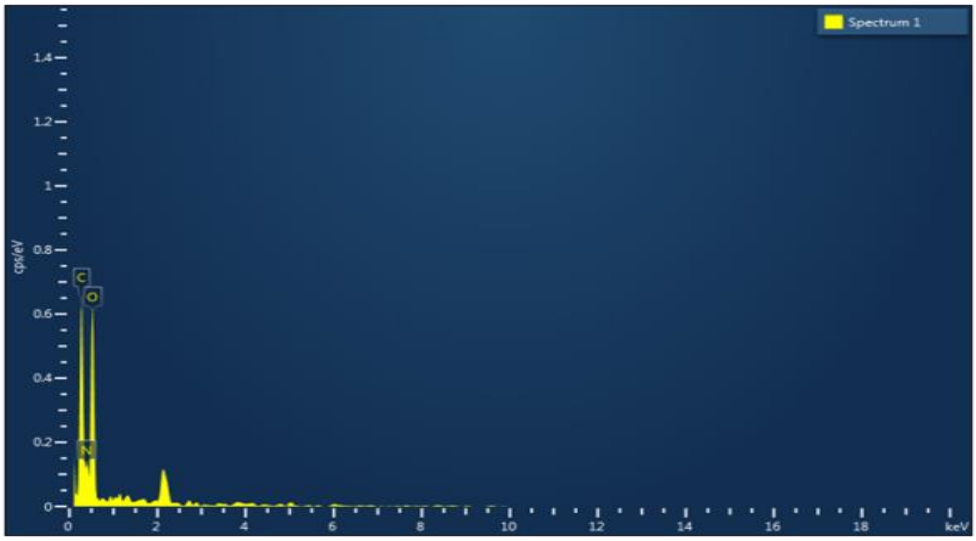

Fig. 14 EDX spectra of LAM crystal

^{1}H FT NMR

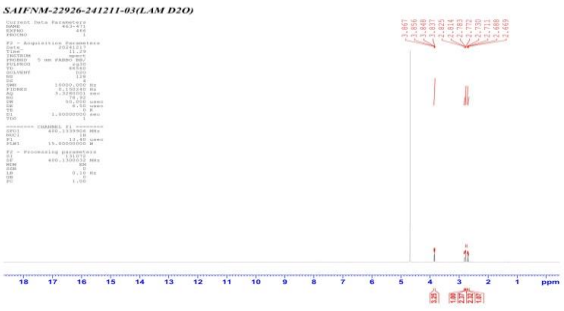

Fig.15 (a).^{1}H FT NMR spectrum of LAM

Received: August 02 2025

International Journal of Applied Mathematics
Volume 38 No. 10s, 2025
ISSN: 1311-1728 (printed version); ISSN: 1314-8060 (on-line version)

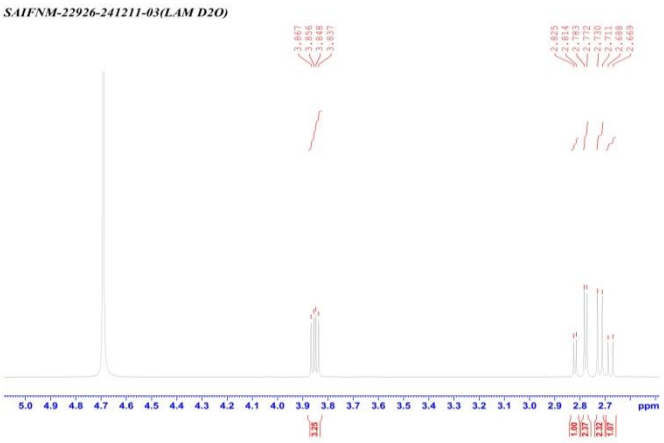

Fig.15 (b).[1]H FT NMR spectrum of LAM

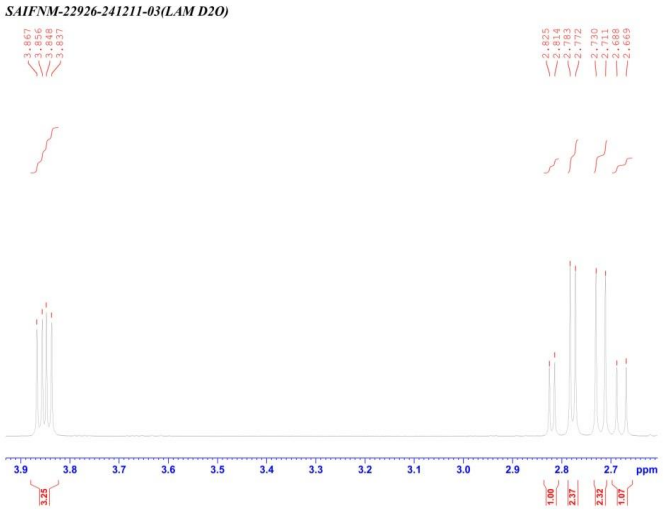

Fig.15 (c).[1]H FT FT NMR spectrum of LAM

[13] C FT NMR

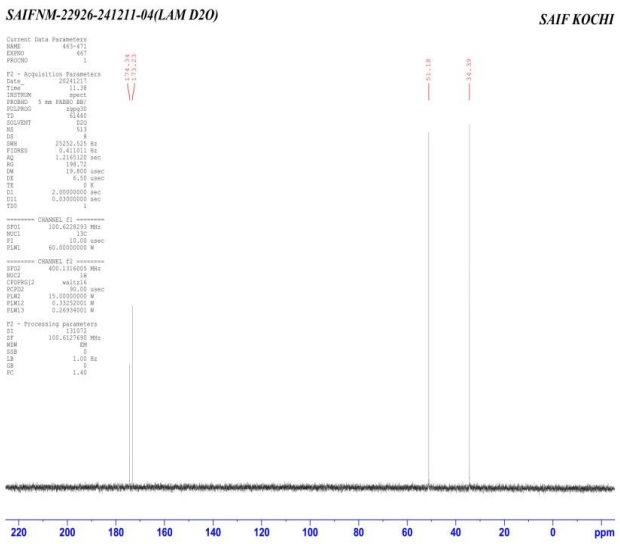

Fig.15 (d) [13]C FT NMR spectrum of LAM

Received: August 02 2025

International Journal of Applied Mathematics
Volume 38 No. 10s, 2025
ISSN: 1311-1728 (printed version); ISSN: 1314-8060 (on-line version)

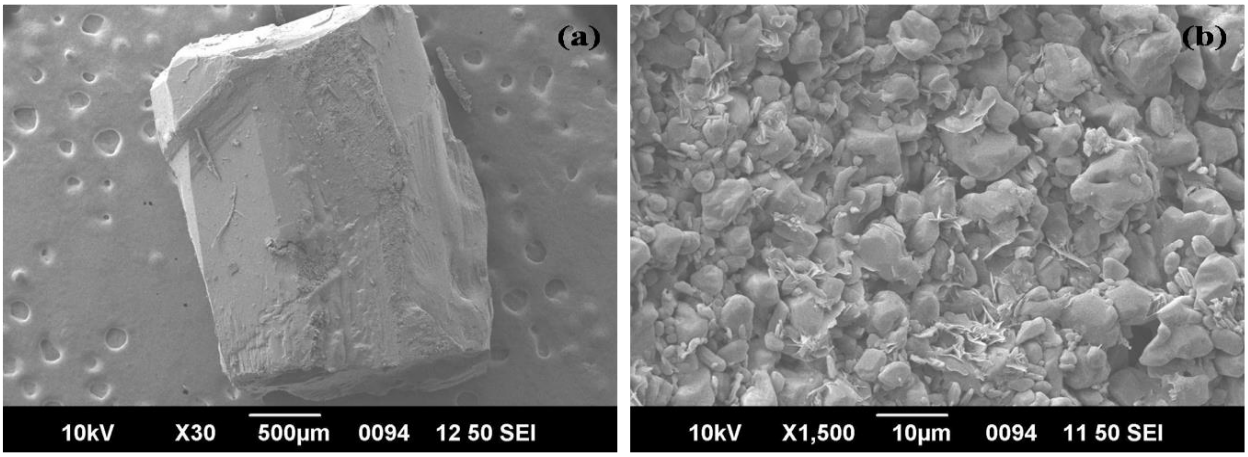

Fig. 16 Morphological image of LAM crystal

Tables

Table 1: Thermal behaviour of LAM crystal

Temp	Temperature T(K)	Slope	E(a) J/mol	Entropy (ΔS) J/mol	Enthalpy (ΔH) J/mol	Gibbs free energy (ΔG) J/mol
Temp 1	1029.25	2521.48575	20966.9	-180.8	12412.5	198512
Temp 2	637.861	2871.31554	23857	-170.2	18553	127154
Temp 3	394.07	1526.94367	12683	-196.1	9410	86670
Temp 4	353.685	6510.79744	54164	-96.8	51228	85463

Table 2: Elemental behaviour of LAM crystal

Elements	Theoretical %	Experimental %
Carbon (C)	31.99 %	**30.90 %**
Hydrogen (H)	6.71 %	**17.76 %**
Nitrogen (N)	18.67 %	**3.79 %**

Table 3: Elements present in the LAM crystal

Received: August 02 2025

International Journal of Applied Mathematics
Volume 38 No. 10s, 2025
ISSN: 1311-1728 (printed version); ISSN: 1314-8060 (on-line version)

Elements	Line type	Weight (%)	Atom (%)
Carbon	K series	36.99	43.28
Nitrogen	K series	11.03	11.06
Oxygen	K series	51.98	45.65
	Total	100	100

Table.4 Standard values of LDT Parametric oscillators of LAM crystal

Sl. No	Parametric oscillators	LDT (GW/cm^2)
1	Optical parametric oscillators	0.1 - 100
2	Second Harmonic Generation	0.1 - 100
3	Third Harmonic Generation	1-50

Table 5: The calculated value of LDT is mentioned of LAM crystals

Compound	SHG Efficiency	Laser damage threshold (GW/cm^2)
KDP	1	0.2
LAM	NIL	24.8

Received: August 02 2025